

<https://doi.org/10.21608/sjsci.2023.172603.1043>

# The Crystallization Kinetic Studies of the $\text{Sn}_5\text{Ge}_{10}\text{Se}_{85-x}\text{Pb}_x$ ( $2.5 \leq x \leq 20$ at. %) Chalcogenide Glasses

M. M. Wakkad, M. M. Abd El Raheem\*, H. A. Mohamed and N. I. Hamed

Physics Department, Faculty of Science, Sohag University, Sohag 82524, Egypt

\*E-mail: [elneh@yahoo.com](mailto:elneh@yahoo.com)

Received: 3<sup>rd</sup> November 2022, Revised: 13<sup>th</sup> December 2022, Accepted: 5<sup>th</sup> January 2023.

Published online: 5<sup>th</sup> February 2023

**Abstract:** The topic of this article concerns the studies of the thermal analysis characterization of the  $\text{Sn}_5\text{Ge}_{10}\text{Se}_{85-x}\text{Pb}_x$  ( $2.5 \leq x \leq 20$  at. %) chalcogenide glass using the differential thermal analysis (DTA) technique. Most of the extracted kinetic parameters in this article focus on the  $\text{Sn}_5\text{Ge}_{10}\text{Se}_{82.5}\text{Pb}_{2.5}$  glass. The obtained DTA thermograms emphasized one endothermic peak characterizing the glass transition process, one exothermic peak characterizing the crystallization process, and lastly, one endothermic peak characterizing the melting of the considered glass. The obtained transformation data of the mentioned glasses are analyzed using the methods of Lasocka and those based on the Johnson-Mehl-Avrami (JMA) formal theory of transformation after modification. Kissinger, Augis, and Bennett (AB), Matusita-Komatsu-Yokota (MKY), and Gao-Wang (GW) methods, in particular. Most of the deduced values of the activation energy of crystallization extracted from the used analytical methods are nearly equal. The crystalline phases of the annealed glass were detected using the X-ray diffraction (XRD) technique. Applying the GW method, it can be emphasized that, the concerned glass is crystallized in two dimensions by surface crystallization. Besides, some of the physical parameters for the considered glass have been calculated, which can be used to ascertain the obtained experimental data. In this context, the average coordination number ( $Z$ ), the deviation of stoichiometry ( $r$ ), the fraction of floppy ( $f$ ), and the overall mean bond energy ( $\langle E \rangle$ ) have been calculated.

**Keywords:**  $\text{Sn}_5\text{Ge}_{10}\text{Se}_{85-x}\text{Pb}_x$ , chalcogenide glass, differential thermal analysis, crystallization kinetics.

## 1. Introduction

The physical properties of chalcogenide materials, especially in their glass form, have attracted much attention due to their wide technical applications [1]. Their physical properties, as known, are strongly influenced by their chemical composition and physical shape [2, 3]. Chalcogenide glass is well-known infrared transmitting materials [4], with inferred transparency in the 3-5 and 8-14 m wavelength ranges. It is recognized that these glass have attracted much attention in the field of electronics as well as in infrared optics since they exhibit several specular phenomena, that are applicable to devices such as electrical switches and/or memory image storage and photoresistors [4-6].

In general, it is recognized that most of the chalcogenide glasses show p-type conduction, and their electrical conductivity is very slightly affected by doping. This insensitivity is attributed to the presence of charged defects, which pin the Fermi level near the mid band [7]. Tohge et al. were the first to point out the role of Bi [8] and Pb [9] modifiers in the appearance of n-type conduction in germanium-chalcogenide glasses. In addition, notable investigations of the electronic conduction processes [10] and the phenomenon of carrier-type reversal [11] in Pb-Ge-Se glasses were reported.

In the last decade, many efforts have been carried out on the physical properties of Pb modification for the ternary Sn-

Ge-Se chalcogenide glasses [12-17]. Kumar et al. [12] have studied the effect of Ge addition on the physical properties of  $\text{Sn}_8\text{Se}_{74}\text{Pb}_{18-x}\text{Ge}_x$  ( $x = 7, 8, 9, 10$  and  $11$  at. %) chalcogenide glasses. They were focused on the calculation of the necessary physical properties, which have an important role in determining the structure and strength of the mentioned glasses. In this context they calculated many of the physical properties of the mentioned glasses. They have calculated the average coordination number, the deviation of stoichiometry, constraints, the overall mean energy, the cohesive energy and the heat of atomization. The authors found that an increasing trend in the overall mean energy, the cohesive energy and the heat of atomization with the Ge addition to the considered glasses. Kumar et al. [13] have studied the basic boundary arrangement and structure of  $\text{Sn}_8\text{Se}_{74}\text{Pb}_{18-x}\text{Ge}_x$  ( $x = 7, 8, 9, 10$ , and  $11$  at. %) chalcogenide glasses. They used thermal analysis and FTIR tools for their studies. The calculated mean bond energy and experimental analysis of the far-infrared spectrum agree with the chemically ordered network model (CONM) and chemical bond approach [14].

Besides, they found that the effect of increasing the concentration of Ge-Se bonds enhances the strength of the glassy network, hence raising the glass transition temperature. Another glass alloy was prepared by Modgil and Rangra [15], where they studied the thermal and optical properties of  $\text{Pb}_9\text{Se}_{71}\text{Ge}_{20-x}\text{Sn}_x$  ( $x = 8, 9, 10, 11$ , and  $12$  at. %) chalcogenide glasses. The thermal analysis parameters were investigated

using the differential scanning calorimetry (DSC) technique in a non-isothermal regime, while the optical parameters were determined using transmittance and reflectivity measurements. They have observed that, the phase separation of the annealed glasses. This observation was confirmed using the x-ray diffraction technique (XRD).

The authors observed that the studied glasses have good forming ability, a high value of glass transition temperature, and glass stability. Besides, they determined many optical parameters, such as the extinction coefficients, the optical band gap, and the refractive index. Thermal and optical measurements revealed that these investigated glasses were influenced by Ge. substitution with Sn, in which the substitution enhances the thermal properties and reduces the optical band gap.

Kumar et al. [16] have studied both, the kinetic properties of  $\text{Sn}_8\text{Se}_7\text{Pb}_{18-x}\text{Ge}_x$  ( $x = 7, 8, 9, 10$  and  $11$  at. %) bulk glasses using the DSC technique and the optical properties of thin films of the mentioned glasses using the spectrophotometry tools. The thermal measurements of the present glasses showed high glass transition temperature and thermal stability. The increase of Ge content in the present glassy matrix caused enhancement in the cross-linking, increased the density of stronger bonds in network and thus offers material applications in high temperatures, such as in thermal imaging and solar cells. The optical properties of the studied glasses reveal the dependence of the optical parameters on matrix composition, their bonding structures and film thickness. All caused a considerable variation of band structure. This is due to the increase of the degree of disorder, density of localized states, and band tailing parameters. Hence, they concluded that the mentioned factors play a pivotal role in tuning the optical properties of the present glasses.

Kumar et al. [17] investigated the dielectric dispersion behaviors of quaternary  $\text{Sn}_8\text{Se}_7\text{Pb}_{18-x}\text{Ge}_x$  ( $x = 7, 8, 9, 10$ , and  $11$  at.%) glassy alloys in the frequency range  $500$  Hz- $1$  MHz and temperature range room temperature to below the glass transition temperature in a notable work. Besides, they studied the temperature variation of DC and AC conductivities and the dielectric parameters of the investigated glasses. They found that the temperature variation of ac conductivity obey the power law  $\omega^s$  where  $\omega$  is the angular frequency and  $s$  is a parameter near unity that decreases or increases according to the ac conduction mechanism. The authors observed a decrease in both dc and ac conductivities with the increase of Ge content. This was attributed to the decrease in the density of localized states and band tailing. In conclusion, they observed the correlation between the dielectric and conductivity behavior of the investigated glasses. The obtained results were interpreted on the basis of the theory of hopping of the charge carriers proposed by Elliot [18]. Because of the importance of chalcogenide alloys in many applied fields mainly optoelectronics, a new series ( $\text{Sn}_5\text{Ge}_{10}\text{Se}_{85-x}\text{Pb}_x$ , where  $x = 2.5, 5, 10, 15, 17.5$ , and  $20$  at.%) of the material is considered in this article. The DTA technique was used to investigate thermal transformation behaviors.

In this context, some of their physical parameters were

calculated such as, the average coordination number ( $Z$ ), the deviation of stoichiometry ( $r$ ), the fraction of floppy ( $f$ ), and the overall mean bond energy ( $E$ ) were calculated. For extracting the kinetic parameters under the non-isothermal regime, the methods of Lasocka [19] and those based on the Johnson-Mehl-Avrami (JMA) formal theory of transformation [20–22] after modification were applied. More specifically, the methods of Kissinger [23], Augis and Bennett (AB) [24], Matusita-Komatsu- (MKY) [25], and Gao-Wang (GW) [26] were utilized.

## 2. Experimental techniques

### 2.1 Bulk Pb-modified.

The usual melt quench technique was used to prepare Sn-Ge-Se ( $\text{Sn}_5\text{Ge}_{10}\text{Se}_{85-x}\text{Pb}_x$ ; where  $x = 2.5, 5, 10, 15, 17.5$ , and  $20$  at%) chalcogenide glasses as described in ref [9]. High-purity element constituents (5N Aldrich) were sealed in an evacuated ( $10^{-5}$  Torr) quartz ampoule. The sealed ampoule was placed in a muffle furnace. To achieve good mixing of the elemental constituents, the furnace temperature was raised with a temperature ramp of about  $3$  K/min and then held at  $1173$  K for about  $24$  hours with continuous rocking. The ingot was finally quenched in ice-cold water. The prepared alloys' glassy nature and crystallised phases of the annealed ingots were investigated using an x-ray diffractometer (Bruker D8 Advance, Germany) with Cu as a target and Ni as a filter ( $\text{Cu } k_1 = 1.5406$ ) at  $30$  kV and  $30$  mA with a scanning speed of  $2.5$  °/min. A calibrated differential thermal analyzer (DTA 50 – Shimadzu Differential Thermal Analyzer - Japan) was used to record the thermograms of the present glassy alloys. For calibration, the melting temperatures and enthalpies of high-purity indium, tin, and lead standards (powder of particle size  $54$  m supplied with the apparatus) were used. The calorimetric sensitivity was  $10$   $\mu\text{W}/\text{cm}$  and the temperature precision was  $\pm 0.1$  K. For each calorimetry measurement (at heating rates  $\beta = 5, 10, 20, 30$ , and  $40$   $\text{K min}^{-1}$ ) typically  $3$  mg of sample in powder form ( $54$   $\mu\text{m}$ ) was sealed in a standard aluminum pan and scanned over a temperature range from room temperature to about  $800$  K. High purity nitrogen gas was used as an inert atmosphere. The values of the glass transition temperature ( $T_g$ ), the onset temperature of crystallization ( $T_c$ ), the peak temperature of crystallization ( $T_p$ ), the end temperature of crystallization ( $T_e$ ), and the melting temperature ( $T_m$ ) of the studied glasses were determined by using the software of the user apparatus.

## 3. Results and discussions

### 3.1 Calculations of some physical parameters

The change in the heat capacity during the glass transition ( $\Delta C_p$ ) for the considered glasses has been calculated using the following equation [27]:

$$\Delta C_p = \Delta H / \beta m \quad (1)$$

where  $\Delta H$  is the change in heat flow through the investigated sample with mass  $m$  at a glass transition and  $\beta$  is the heating rate. The average coordination number  $Z$  of the considered glasses has been calculated using the standard procedures

described elsewhere [28] using the coordination numbers (CN) of 4, 4, 2, and 4 for Sn, Ge, Se, and Pb, respectively. Thus, for  $\text{Sn}_a\text{Ge}_b\text{Se}_c\text{Pb}_d$  ( $a + b + c + d = 1$ ) glasses, the values of  $Z$  could be given by:

$$Z = a\text{CN}(\text{Sn}) + b\text{CN}(\text{Ge}) + c\text{CN}(\text{Se}) + d\text{CN}(\text{Pb}) \quad (2)$$

The calculated values of  $Z$  for the studied glasses are recorded in **Table 1**. The parameter  $r$  which determines the deviation of the stoichiometry of the studied glasses and is expressed by the ratio of the covalent bonding possibilities of chalcogen atoms to those of non-chalcogen atoms has been calculated using the following formula [29, 30]:

$$r = c\text{CN}(\text{Se}) / (a\text{CN}(\text{Sn}) + b\text{CN}(\text{Ge}) + d\text{CN}(\text{Pb})) \quad (3)$$

The calculated values of  $r$  of the mentioned glasses are given in **Table 1**.

The bond energies ( $E_{AB}$ ) of heteropolar A-B bonds can be estimated using the following Pauling's equation [31]:

$$E_{AB} = 0.5(E_{AA} + E_{BB}) + 23(X_A - X_B)^2 \quad (4)$$

where  $E_{AA}$  and  $E_{BB}$  and  $X_A$  and  $X_B$  are, respectively, the homopolar bond energies and electronegativity of A and B atoms. The homopolar bond energies and electronegativity are obtained from Reference [32, 33].

The overall mean bond energy ( $\langle E \rangle$ ) of the present glasses, which were found [30] to depend on the average coordination number  $Z$ , the degree of cross-linking/atom ( $P$ ), the type of bonds, and the bond energy forming a network, has been calculated as described by Tichy and Ticha [30]. Values of  $\langle E \rangle$  have been recorded in Table 1 too. Values of the fraction of floppy ( $f$ ) of the present glasses, which are recorded in Table 1, have been calculated according to the theory of M.F. Thorpe [34].

**Table 1:** shows the relationship between the physical parameters  $Z$ ,  $r$ ,  $f$ , and  $E$  of  $\text{Sn}_5\text{Ge}_{10}\text{Se}_{85-x}\text{Pb}_x$  glasses and their chemical composition  $x$ .

X	Z	R	f	$\langle E \rangle$ kJ mol <sup>-1</sup>	$\langle E \rangle$ eV atom <sup>-1</sup>
2.5	2.35	2.357	0.04167	206.558	2.141
5	2.40	2	0	207.192	2.148
10	2.50	1.500	-0.08333	207.676	2.153
15	2.60	1.167	-0.16667	207.052	2.146
17.5	2.65	1.038	-0.20833	206.420	2.140
20	2.70	0.929	-0.25	92.560	0.959

Looking at the recorded  $Z$  values in **Table 1** it can be seen that, the considered compositions undergo two topological changes. Really, the topological model is based on the constraint theory [34, 35] and structural dimensionality consideration [28]. In this model, the properties can be discussed in terms of the average coordination number  $Z$ , which is independent of the valence bond species. Two topological thresholds at the average coordination numbers  $Z \approx 2.4$  and  $Z \approx 2.67$  have been predicted by this model. At  $Z \approx 2.4$  (in the present case, composition with  $x = 5$  at. %) the glass network has a mechanical threshold or critical composition, at which the network changes from an elastically floppy

(polymeric glass) type to a rigid (amorphous solid) type [34, 35]. The recorded data of the fraction of floppy  $f$  [34] in Table 1 confirm this glass structure transition. Looking at the recorded  $f$  data, it can be emphasized that, for the glass composition with  $x = 2.5$  at. % it is observed that this glass has  $f = 0.04167$  meaning value. When  $x = 5$  at. %,  $f = 0$  and when  $x$  is greater than 5 at. %,  $f$  has meaningless value. Extending the topological model to the medium-range structures, another topological feature at  $Z \approx 2.67$  (compositions with  $x = 17.5$  and 20 at. %) was observed. This feature was attributed to a change from a two-dimensional (2D) layered structure to a three-dimensional (3D) network arrangement due to cross-linking [28]. This information will be used later when we talk about the results of thermal analysis.

### 3. Results and Discussion:

#### 3.2. X-ray diffraction (XRD) measurements and phase transition temperatures

The XRD of the bulk  $\text{Sn}_5\text{Ge}_{10}\text{Se}_{85-x}\text{Pb}_x$  ( $2.5 \leq x \leq 20$  at. %) chalcogenide alloys is shown in Fig. 1. The absence of any sharp peaks confirms the glassy nature of the considered alloys. Except for the compositions with  $x = 15$  and 17.5 at. %, which have small peaks. These emerging characterizing peaks of the glasses with  $x = 15$  and 17.5 at. were for the Ge, SnSe, GeSe, and PbSe crystalline phases, respectively. The mentioned diffractograms of the studied glasses emphasize that there are three halos; the first two moderate halos are in the  $2\theta$  range of  $10^\circ - 17.5^\circ$  and  $22.5^\circ - 35^\circ$  and the third, which is weak, is in the  $2\theta$  range of  $45^\circ - 57.5^\circ$ . These observations may give us the impression that the glassy alloys will crystallize with heat treatment into different crystalline phases.

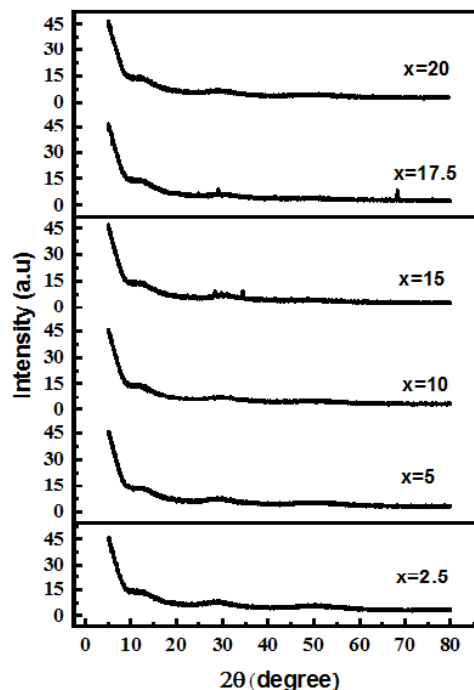


**Fig. 1:** X-ray diffraction patterns of as-prepared  $\text{Sn}_5\text{Ge}_{10}\text{Se}_{85-x}\text{Pb}_x$  ( $2.5 \leq x \leq 20$  at. %) compositions.

The thermograms of the  $\text{Sn}_5\text{Ge}_{10}\text{Se}_{85-x}\text{Pb}_x$  (2.5 x 20 at%) chalcogenide glasses were measured using differential thermal analysis (DTA) at a heating rate of = 5 K min<sup>-1</sup>. The obtained DTA thermograms look like the observed standard ones. The thermograms have three thermal transition events. The first event is the existence of one endothermic, which characterizes the glass transition temperature and confirms that the mentioned glasses have one structural phase. The second event is the existence of one exothermic peak characterizing the crystallization process of the studied glasses. This behavior may mean that the undertaken chalcogenide glasses do not split into their binary phases. The third event is the existence of one endothermic peak that characterizes the melting point of these glasses. These observations give us an impression that the glasses under study are one-phase alloy. Table 2 contains the phase transition temperatures of the mentioned  $\text{Sn}_5\text{Ge}_{10}\text{Se}_{85-x}\text{Pb}_x$  (2.5 ≤ x ≤ 20 at %) chalcogenide glasses ( $\beta = 5 \text{ K min}^{-1}$ ) and some of the extracted thermal parameters.

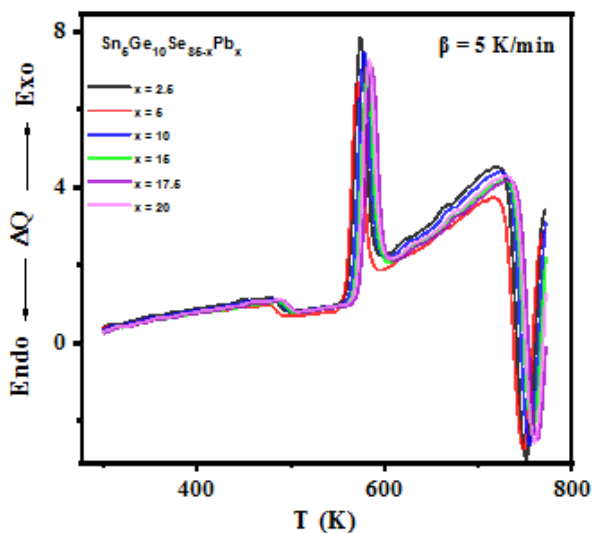


**Fig. 2:** The DTA thermograms measured at heating rate  $\beta = 5 \text{ K min}^{-1}$  of the  $\text{Sn}_5\text{Ge}_{10}\text{Se}_{85-x}\text{Pb}_x$  (2.5 ≤ x ≤ 20 at %) chalcogenide glasses.

**Fig. 3** shows the dependence of  $T_g$ ,  $T_p$  and  $T_m$  on the composition of the studied  $\text{Sn}_5\text{Ge}_{10}\text{Se}_{85-x}\text{Pb}_x$  (2.5 ≤ x ≤ 20 at %) glasses. Looking to the presented data in the mentioned graph gives us an impression that, there are small kink in  $T_g$  curve at  $x = 17.5 \text{ at. \%}$  and for  $T_p$  and  $T_m$  curves at the compositions with  $x = 5$  and  $17.5 \text{ at. \%}$ . These observations may be attributed to the structural changes of the present compositions, where at  $x = 5 \text{ at. \%}$  the network changes from an elastically floppy (polymeric glass) type to a rigid (amorphous solid) type [34, 35]. The second small kink may be attributed to changes from a two-dimensional 2D layered structure to a three-dimensional 3D network arrangement due to cross-linking [28].

To detect the emerging crystalline phases of the present  $\text{Sn}_5\text{Ge}_{10}\text{Se}_{85-x}\text{Pb}_x$  (2.5 ≤ x ≤ 20 at %) glasses through the thermal analysis process, they were annealed at a temperature higher than the end of the exothermic peak, definitely at 703 K.

**Table 2:** Phase transition temperatures and some extracted kinetic parameters of the  $\text{Sn}_5\text{Ge}_{10}\text{Se}_{85-x}\text{Pb}_x$  (2.5 ≤ x ≤ 20 at %) chalcogenide glasses, extracted from DTA thermograms measured at heating rate  $\beta = 5 \text{ K min}^{-1}$ .

x	$T_g$ (K)	$T_c$ (K)	$T_p$ (K)	$T_m$ (K)	$T_m$ (K)	$\Delta T$ (K)	$H_f$	$k_{eff}$	$\Delta H$	$\Delta C_p$	F
2.5	475.68	551	574.5	597	751	75.32	0.3766	0.274	0.3518	23.453	0.1670
5	477	548	572	594	747	71	0.3568	0.263	0.3084	---	---
10,00	483.00	554	579	604	756	71	0.3515	0.260	0.3286	---	---
15	486	557	581	606	759	71	0.3515	0.260	0.2899	---	---
17.5	492	563	586	610	763	71	0.3550	0.262	0.3194	---	---
20	489	558	583	607	761	69	0.3399	0.254	0.3102	---	---

Here – for abbreviation – we only present the x- ray diffraction patterns of the  $\text{Sn}_5\text{Ge}_{10}\text{Se}_{85-x}\text{Pb}_x$  glasses ( $x = 2.5, 10$  and  $20 \text{ at. \%}$ ) annealed at 703 K for 2 hrs. The mentioned diffractograms are shown in **Figs. 4, 5, and 6** respectively. Looking at the data of the diffractograms shown in **Figs. 4, 5 and 6** give us an impression that all annealed glasses show the crystalline peaks of the SnSe, SnSe<sub>2</sub>, GeSe, GeSe<sub>2</sub>, PbSe and PbSe<sub>2</sub> crystalline phases. Accordingly, the thermal analysis studies will be abbreviated by considering only one composition. In this context, the first composition of the studied glasses is considered, viz; the  $\text{Sn}_5\text{Ge}_{10}\text{Se}_{82.5}\text{Pb}_{2.5}$  glass.

**Fig. 7** shows the DTA thermograms of the  $\text{Sn}_5\text{Ge}_{10}\text{Se}_{82.5}\text{Pb}_{2.5}$  chalcogenide glass, those measured at different heating rates  $\beta$  in the range of 5 – 40 K min<sup>-1</sup>. The obtained thermograms have elucidated the usual thermal events recorded in these studies. The observations reveal that, all recorded values of  $T_g$ ,  $T_c$ ,  $T_p$  and  $T_m$  behave in the usual manner, which has increased with the increase of the heating rate. The obtained values of phase transition temperatures and some of the extracted thermal kinetic parameters are recorded in Table 3. Mainly, the obtained phase transition temperatures agreed with those obtained previously [15, 16]. Using these data gives us most of the kinetic parameters concerning the considered glasses. In this context, it can extract the values of glass stability, glass forming ability, fragility, the Lasocka parameters, the activation energy of glass transition, the activation energy of crystallization, the kinetic exponent and, the dimensionality of crystallization growth.



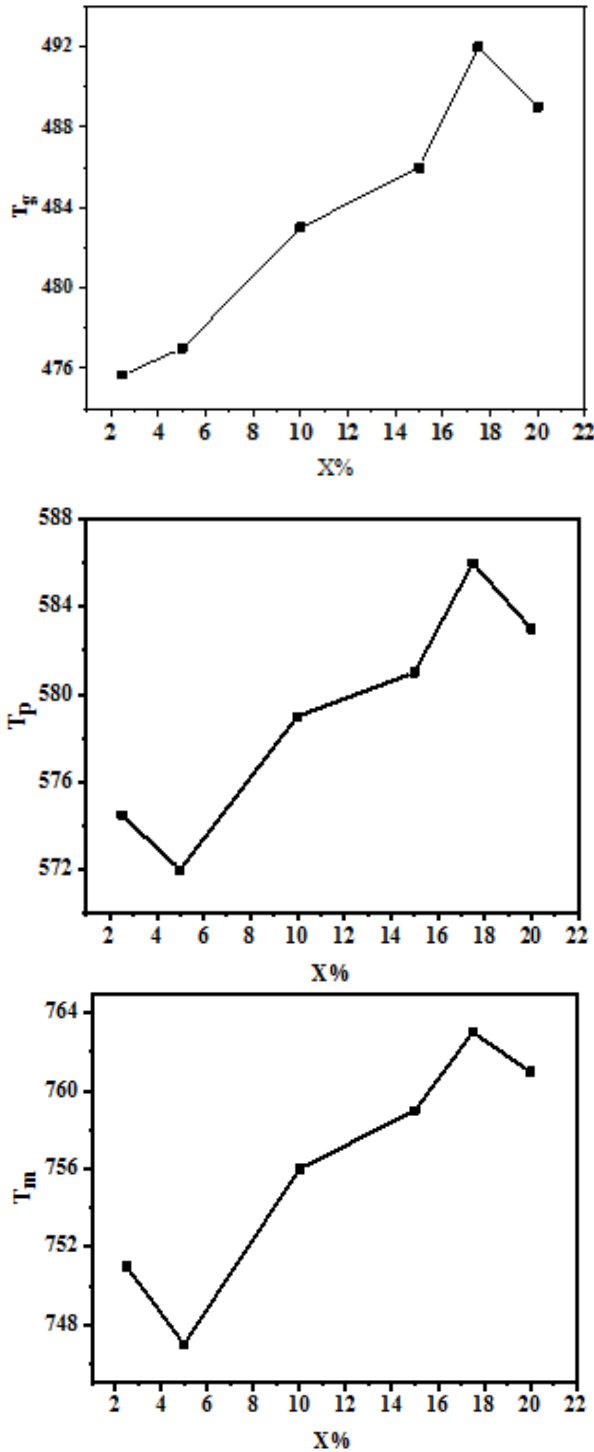


**Fig. 3.** The variations of  $T_g$ ,  $T_p$  and  $T_m$  with the glass composition of the of  $Sn_5Ge_{10}Se_{85-x}Pb_x$  ( $2.5 \leq x \leq 20$  at %) chalcogenide glasses and the thermogram measured at  $\beta = 5 K min^{-1}$

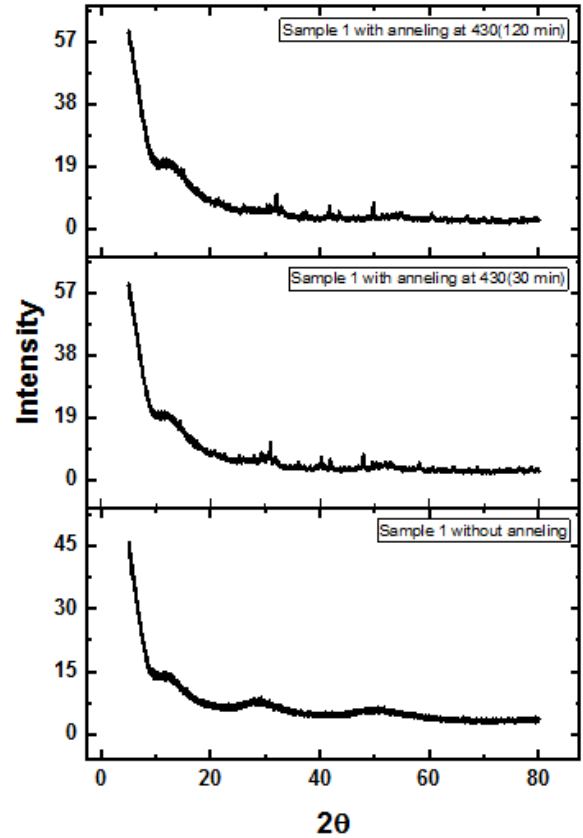


**Fig. 4:** X-ray diffraction patterns for  $Sn_5Ge_{10}Se_{82.5}Pb_{2.5}$  glass, as prepared and annealed at 703 K for 2 hrs.

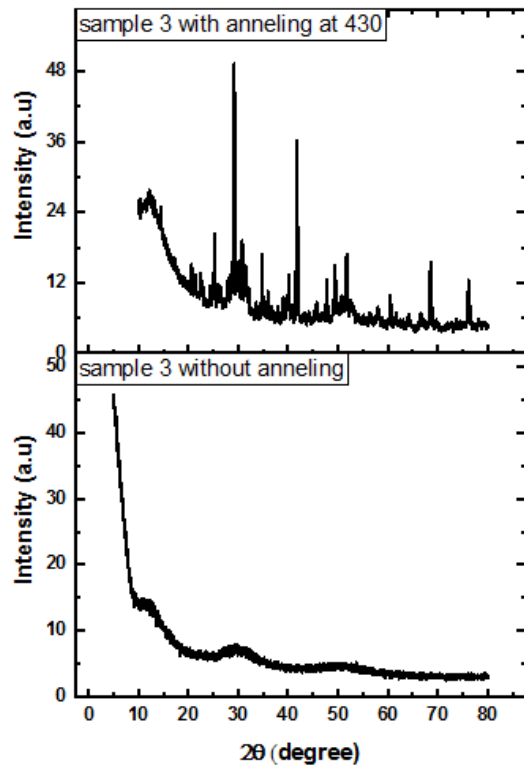


**Fig. 5:** X- ray diffraction patterns for  $Sn_5Ge_{10}Se_{75}Pb_{10}$  glass, as- prepared and annealed at 703 K for 2 hrs.

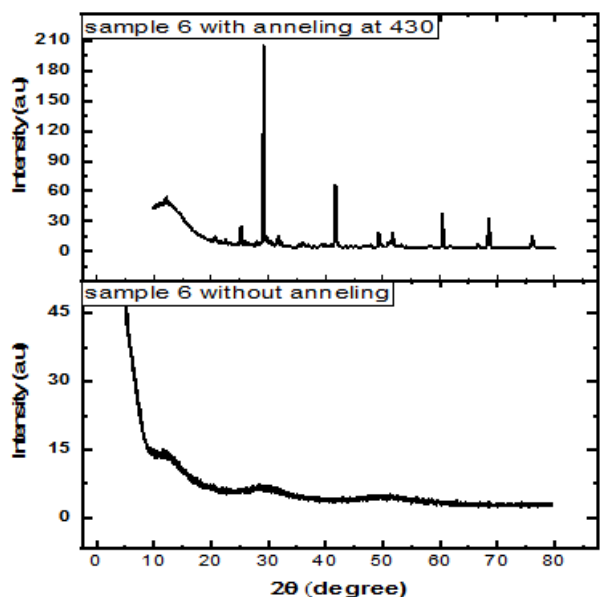


Fig. 6: X- ray diffraction patterns for Sn<sub>5</sub>Ge<sub>10</sub>Se<sub>65</sub>Pb<sub>20</sub> glass, as- prepared and annealed at 703 K for 2 hrs.

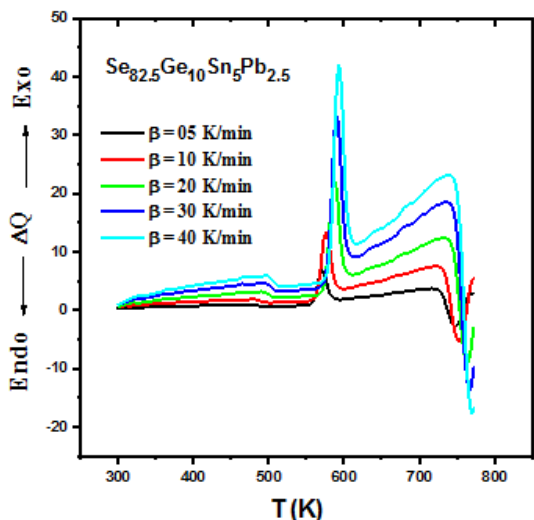


Fig. 7. The DTA thermogram of the Sn<sub>5</sub>Ge<sub>10</sub>Se<sub>82.5</sub>Pb<sub>2.5</sub> chalcogenide glass. The thermogram was measured at different heating rates in the range of 5 – 40 K min<sup>-1</sup>.

### 3.2. Thermal stability and glass formation factors

The important parameter which employed to estimate the glass stability is the thermal stability ( $\Delta T$ ), which is defined as  $\Delta T = T_c - T_g$  [36]. The obtained values of  $\Delta T$  are recorded in Tables 2 and 3. Another parameter introduced by Hruby and Stourac [37] is the glass forming ability ( $H_r$ ) which is defined by the following relation:

$$H_r = \Delta T / (T_m - T_c) \quad (5)$$

Accordingly [37], when  $H_r \leq 0.1$  good glass forming cannot be obtained. Looking to the recorded data of  $H_r$  in Tables 2 and 3, which they are approximately in the range of 0.35, emphasized that the studied alloys are good glasses.

Table 3: Phase transition temperatures and some extracted kinetic parameters of the Sn<sub>5</sub>Ge<sub>10</sub>Se<sub>82.5</sub>Pb<sub>2.5</sub> glass, extracted from their DTA thermograms, those measured at different heating rates  $\beta$  in the range of 5 – 40 K min<sup>-1</sup>.

$\beta$ (Kmin <sup>-1</sup> )	$T_g$ (K)	$T_c$ (K)	$T_p$ (K)	$T_e$ (K)	$T_m$ (K)	$\Delta T$ (K)	$H_r$	$k_{gl}$	$\Delta H$	$\Delta C_p$	$F$
5.00	475.68	551	574.5	597	751	75.32	0.3766	0.274	0.3518	23.453	0.1670
10	484	554	576	601	753	70	0.35176	0.260	0.5676	18.920	0.1668
20	492	562	588	613	764	70	0.34653	0.257	1.0268	17.113	0.1641
30	494.50	566	591	616	767	71.5	0.35572	0.262	1.5438	17.153	0.1633
40	495.70	568	593	619	770	72.3	0.35792	0.264	1.9378	16.148	0.1626

Furthermore, the glass formation factor ( $k_{gl}$ ) [37] is among the parameters which can give information about the thermal stability and glass forming ability of the glasses. The higher values of  $k_{gl}$  reflect the greater thermal stability and glass forming ability of the studied glasses. The glass formation factor  $k_{gl}$  is given by the following formula:

$$k_{gl} = \Delta T / (T_m - T_g) \quad (6)$$

The obtained values of  $k_{gl}$  of the studied compositions are recorded in Tables 2 and 3 too. These recorded values of  $k_{gl}$  emphasized that, good glass formation and thermal stability of the considered alloys [37]. Also, there is a glass parameter which is called the fragility ( $F$ ). This glass parameter characterizes and quantifies the anomalous non- Arrhenius transport behavior of glassy materials as they approach the ergodicity-breaking glass transition [38-40]. Fragile glasses are substances with non-directional interatomic/ inter molecular bonds. Strong glasses are those which show resistance to structural degradation and usually associated with small  $\Delta C_p$ . The fragility was calculated using the following relation [41]:

$$F = E_t / T_g \ln 10 \quad (7)$$

where  $E_t$  is the estimated activation energy for glass transition in units of temperature and evaluated using Kissinger formula [23]. The extracted values of  $F$  for the studied Sn<sub>5</sub>Ge<sub>10</sub>Se<sub>85-x</sub>Pb<sub>x</sub> (2.5 ≤ x ≤ 20 at %) glasses are recorded in Tables 2 and 3. The recorded values of fragility of the present glasses seem to be low. Accordingly [42, 43], low values of  $F$  mean that the studied glasses are strong glass-forming liquids.

### 3.3. Dependence of $T_g$ on the heating rate

To study the variation of  $T_g$  with the heating rate  $\beta$ , it can be using two methods; the first method which is called the Lasocka approach [19], which has the following form:

$$T_g = A + B \ln \beta \quad (8)$$

where A and B are constants for a given glass composition. Really, the value of the constant A is equal to the glass transition temperature at heating rate  $\beta = 1$ , while the constant B determines the response of configurational change within the glass transition region to the heating rate [19].

The plot of  $T_g$  vs.  $\ln \beta$  for the studied  $\text{Sn}_5\text{Ge}_{10}\text{Se}_{82.5}\text{Pb}_{2.5}$  glass is shown in Fig.8. The extracted values of A and B are recorded in Table 4.

**Table 4:** Values of A, B and  $E_t$  for the studied  $\text{Sn}_5\text{Ge}_{10}\text{Se}_{82.5}\text{Pb}_{2.5}$  chalcogenide glass.

Composition	A (K)	B (min)	$E_t$ (kJ/mol)
$\text{Sn}_5\text{Ge}_{10}\text{Se}_{82.5}\text{Pb}_{2.5}$	460.73	9.88	185.885

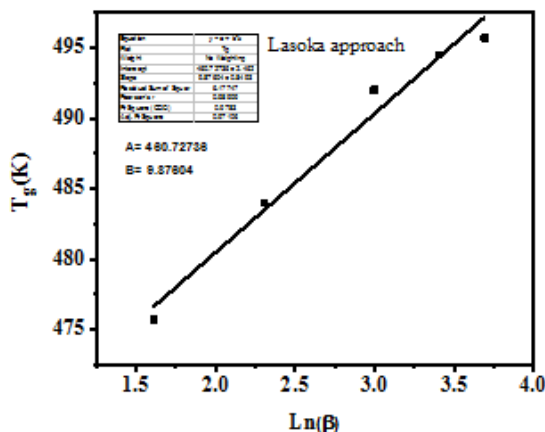


**Fig. 8:** Lasocka  $T_g$  vs.  $\ln \beta$  graph for the studied  $\text{Sn}_5\text{Ge}_{10}\text{Se}_{82.5}\text{Pb}_{2.5}$  chalcogenide glass.

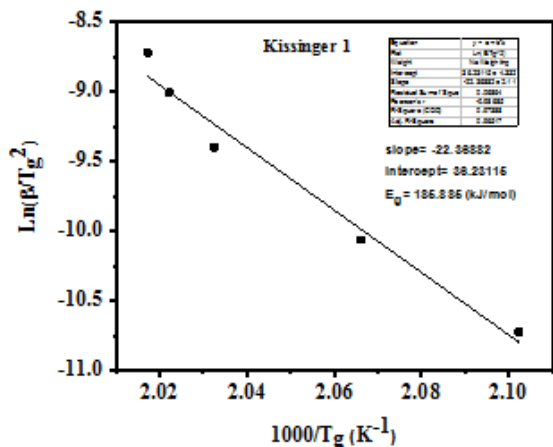


**Fig. 9:** Kissinger  $\ln(\beta / T_g^2)$  vs.  $1 / T_g$  graph for the considered  $\text{Sn}_5\text{Ge}_{10}\text{Se}_{82.5}\text{Pb}_{2.5}$  chalcogenide glass.

The obtained value of the constant A (the glass transition temperature at heating rate  $\beta = 1$ ) well matches the experimentally obtained data of glass transition temperature, that is recorded in Tables 2 and 3. Besides, the obtained value of B matches those obtained previously [15,16] for chalcogenide glass series resemble the present glass. The second method to study the variation of  $T_g$  with the heating rate  $\beta$ , is the application of Kissinger formula [23] (this formula is derived to calculate the activation energy of crystallization) to extract the value of the activation energy of glass transition ( $E_t$ ). The mentioned Kissinger formula in this task has the following form:

$$\ln(\beta / T_g^2) = -E_t / (RT_g) + \text{const.} \quad (9)$$

where R is the universal gas constant ( $8.3145 \text{ JK}^{-1}\text{mol}^{-1}$ ). The plot of  $\ln(\beta / T_g^2)$  vs.  $1/T_g$  is depicted in Fig. 9. The extracted  $E_t$  value from the slope of Fig. 9 is recorded in Table 4 too. Really, the obtained  $E_t$  value of the considered glass is approximately in agreement with those recorded previously for a resemble chalcogenide glasses [15, 16].

### 3.4. Activation energy of crystallization

In this part, four standard methods have been used to determine the activation energy of crystallization ( $E_c$ ) of the considered  $\text{Sn}_5\text{Ge}_{10}\text{Se}_{82.5}\text{Pb}_{2.5}$  chalcogenide glass. These methods were based on the Johnson-Mehl-Avrami (JMA) formal theory of transformation [20-22] after some modification. More specifically, the methods of Kissinger [23], Augis and Bennett (AB) [24], Matusita-Komatsu-Yokota (MKY) [25] and Gao-Wang (GW) [26] have been used.

#### 3.4.1 Kissinger method

The first method, which has been used to determine the activation energy of crystallization  $E_c$  is Kissinger method [23]. In this method the peak temperature of crystallization  $T_p$  is related to the heating rate  $\beta$  according to the following relation :

$$\ln(\beta/T_p^2) = -E_c/(RT_p) + \ln(E_c/RK_0) \quad (10)$$

where  $K_0$  is the frequency factor which measures the probability of effective molecular collisions for the formation of the activated complexes in each case. From Kissinger  $\ln(\beta / T_p^2)$  and  $1 / T_p$  plot shown in Fig. 10, the values of  $E_c$  and  $K_0$  were evaluated by least squares fitting method. The extracted values of  $E_c$  and  $K_0$  are recorded in Table 5.

**Table 5:** The extracted values of the  $E_c$  and the frequency factor  $K_0$  deduced from Kissinger and Augis-Bennett methods of the considered  $\text{Sn}_5\text{Ge}_{10}\text{Se}_{82.5}\text{Pb}_{2.5}$  chalcogenide glass.

Composition	$E_c$ - Kissinger (kJ·mol <sup>-1</sup> )	$K_0$ (K)	$E_c$ - Augis and Bennett (kJ·mol <sup>-1</sup> )
$\text{Sn}_5\text{Ge}_{10}\text{Se}_{82.5}\text{Pb}_{2.5}$	257.710	$5.786 \times 10^{-15}$	257.423

3.4.3. Matusita-Komatsu-Yokota (MKY) method

The theoretical basis for interpreting the thermal analysis data in non-isothermal kinetics- as mentioned previously- is provided by the formal theory of transformation kinetics developed by Johnson-Mehl-Avrami (JMA) [20-22]. It is known that, the volume fraction crystallized ( $x$ ) at a given temperature  $T$ , is given by  $x = A_T/A$ , where  $A$  is the total area of the exotherm between the temperature of beginning of crystallization  $T_c$  and the temperature at which the crystallization process is completed  $T_e$  and  $A_T$  is the area between  $T_c$  and  $T$ . According to Handerson [45] and Malek [46] the check of the validity of JMA formal theory of transformation kinetics in non-isothermal regime is the volume fraction crystallized  $x$  at the peak temperature of crystallization  $T_p$  should be in the range of 0.62 – 0.64 and it weakly dependent on the heating rate. In the present thermal analysis study the  $x$  values change in the range of 0.55- 0.65 and slightly dependent on the heating rate. Accordingly, one of the methods based on JMA formal theory of transformation kinetics now have been applied. Here, the method of Matusita et al. (MKY) [25] is chosen to analyze our obtained thermal analysis data.

In MKY method - for non-isothermal kinetics - the volume fraction  $x$  of the crystal precipitated in the glass heated at a uniform heating rate  $\beta$  is related to  $E_c$  through the following relation [25]:

$$\ln[-\ln(1-x)] = -n \ln \beta - 1.052 m E_c / RT_p + const. \tag{12}$$

where  $n$  and  $m$  are numerical factors depending on the nucleation process and growth morphology of the crystal [25]. It's known that, the values of  $n$  may be 4, 3, 2 or 1, which are related to the different glass-crystal transformation mechanisms. In the other side, values of  $m$  must be 3, 2 and 1 which corresponds to three-dimensional, two dimensional and one-dimensional growth, respectively [36]. When nuclei formed during the heating at constant rate are dominant  $n = (m+1)$  and when nuclei formed in the previous heat treatment before thermal analysis are dominant  $n = m$  [47]. Then, for the present study  $n = (m+1)$ .

Fig. 12 displays the  $\ln[-\ln(1-x)]$  vs.  $1/T_p$  plot, at different heating rates in the range of 5-40  $K\ min^{-1}$ , for the exothermic crystallization peaks of  $Sn_5Ge_{10}Se_{82.5}Pb_{2.5}$  chalcogenide glass. The observation of the present data indicating that, saturation of nucleation sites in the final stage of crystallization [48] or restriction of crystal growth by small size of the particles [49]. Accordingly [36], the data analysis, where there is a change in the slope, is confined to the initial linear region. The values of  $mE_c$  at different heating rates can be obtained from the slope of Fig. 12. The values of  $mE_c$  seemed to be slightly dependent on  $\beta$ . Hence, it can be considered the average value of  $mE_c$ , calculated and recorded in Table 6.

To find the kinetic parameter  $n$ , the elucidated data in Fig. 12 can be used to calculate the dependence of  $\ln[-\ln(1-x)]$  on the  $\ln\beta$ . This was done at two different temperatures namely 574 and 576 K. Hence, the last collected data are plotted in the form of  $\ln[-\ln(1-x)]$  vs.  $\ln\beta$  as shown in Fig. 13.

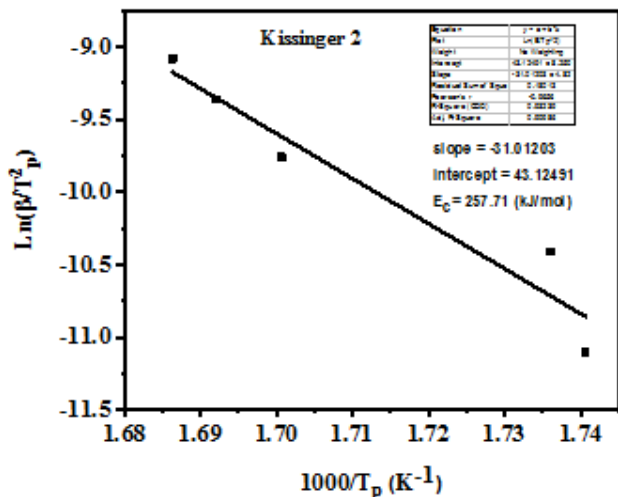


Fig.10: Kissinger  $\ln(\beta/T_p^2)$  vs.  $1/T_p$  plot for the  $Sn_5Ge_{10}Se_{82.5}Pb_{2.5}$  chalcogenide glass.

3.4.2. Augis and Bennett's method

The second method, which has been used to determine the activation energy of crystallization, is the most precise method [44], viz; the Augis and Bennett method [24]. This method relates the peak temperature of crystallization  $T_p$  with the heating rate  $\beta$  according the following relation:

$$\ln[\beta(T_p - T_0)] = -E_c / RT_p + const. \tag{11}$$

where  $T_0$  is the room temperature (300 K). Fig. 11 shows the Augis and Bennett  $\ln[\beta/(T_p - T_0)]$  vs.  $1/T_p$  plot for the  $Sn_5Ge_{10}Se_{82.5}Pb_{2.5}$  chalcogenide glass. Fitting the data in the mentioned figure give us the value of  $E_c$  which is recorded in Table 5 too. Mainly it is clear that, the deduced  $E_c$  values from the Kissinger and Augis-Bennett methods are approximately equal and in agreement with those recorded previously for a resemble chalcogenide glasses [15, 16].

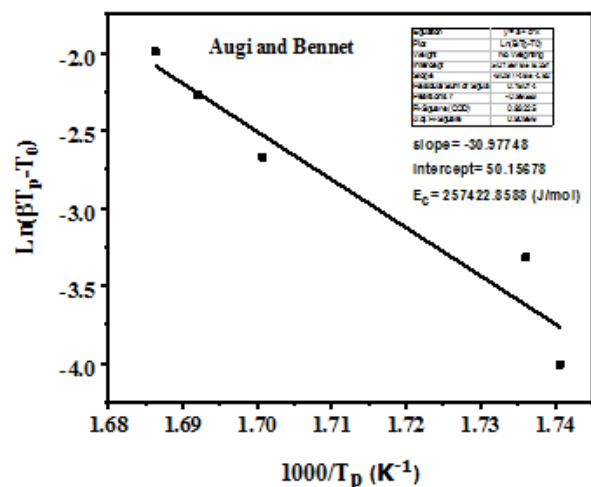


Fig. 11: Augis-Bennett  $\ln[\beta/(T_p - T_0)]$  vs.  $1/T_p$  plot for the  $Sn_5Ge_{10}Se_{82.5}Pb_{2.5}$  chalcogenide glass.



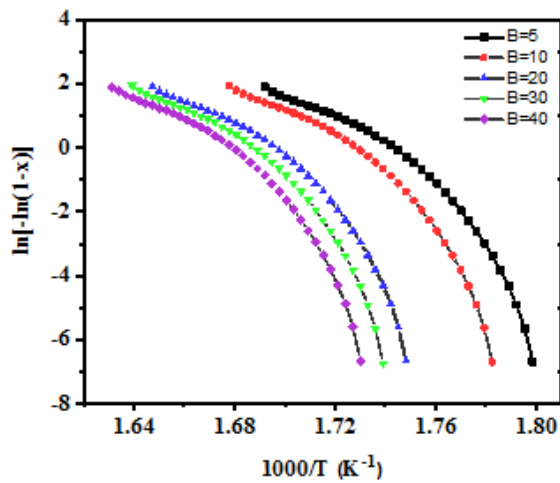


Fig. 12. The  $\ln [-\ln(1-x)]$  vs.  $1/T_p$  plot for the  $\text{Sn}_5\text{Ge}_{10}\text{Se}_{82.5}\text{Pb}_{2.5}$  chalcogenide glass taken at different heating rate.

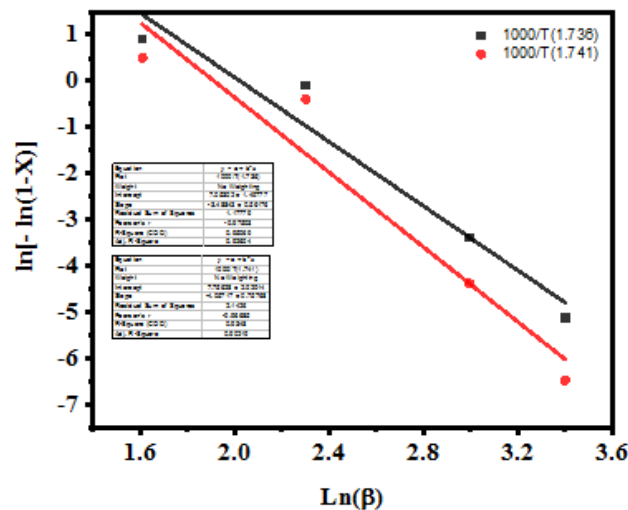


Fig. 13. The plot of  $\ln [-\ln(1-x)]$  vs.  $\ln\beta$  for the  $\text{Sn}_5\text{Ge}_{10}\text{Se}_{82.5}\text{Pb}_{2.5}$  chalcogenide glass at the temperatures 574 and 576 K.

The extracted  $n$  value determined from the slope of the last figure, at temperatures 574 and 576 K, are equal to 4.06 and 3.49, respectively. It has been observed that these values are not integers. Then it has been recognized that more than one mechanism participate in crystal growth [25]. The mean value of  $n = 3.78 \approx 4$ , hence the value of  $m \approx 3$ . Accordingly, the crystal growth of the present glass is grown in three dimensions. Using the obtained value for  $m$ , the value of  $E_c$  can be extracted from the MKY method. The values of  $n$ ,  $m$  and  $E_c$  are recorded in Table 6. The extracted  $E_c$  value from the MKY method is more than twice of the obtained values from the Kissinger and Augis-Bennett methods. This may be attributed to that, the used relations in these three methods apply different approximations in their derivations, or the deviation of our thermal analysis data from Handerson [45] and Malek [46] criterion to the validity of the modified JMA formal theory of transformation kinetics in non-isothermal

regime (specifically the MKY method). Therefore, at this stage of our study, we exclude the obtained results from the MKY method.

Table 6: The values of the average of  $m E_c$ ,  $n$ ,  $m$  and  $E_c$  deduced from the MKY method of the considered  $\text{Sn}_5\text{Ge}_{10}\text{Se}_{82.5}\text{Pb}_{2.5}$  chalcogenide glass.

Composition	The average of $m E_c$ $\text{kJmol}^{-1}$	$n$	$m$	$E_c$ - JMA $\text{kJmol}^{-1}$
$\text{Sn}_5\text{Ge}_{10}\text{Se}_{82.5}\text{Pb}_{2.5}$	2018.40	$3.78 \approx 4$	$\approx 3$	672.80

3.4.4. The method of Gao-Wang (GW)

In this part, the method of Gao-Wang [26] is applied to our obtained thermal analysis data. The important graph needed in this method is the plot representing the variation of the crystallization fraction  $x$  with the temperature, at different heating rate, which is shown in Fig. 14. This reveals the typical sigmoid curve as a function of temperature. In the other side, it is known that the ratio between the ordinate, at any temperature, of the exotherm of the thermal analysis curve and its total area gives the corresponding crystallization rates  $(dx/dt)T$ , which makes it possible to build the curves of the exothermic peaks [26]. These curves are shown in Fig. 15.

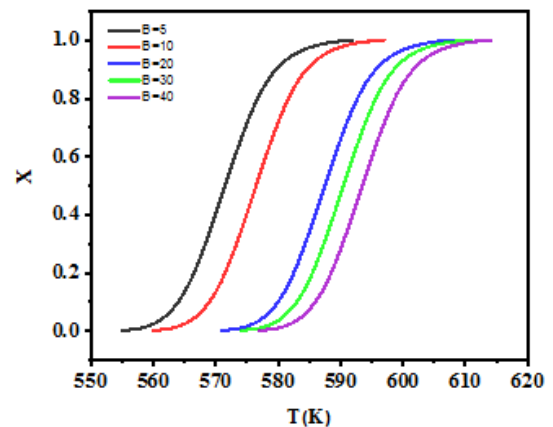


Fig. 14. The crystallization fraction  $x$  as a function of temperature, at different heating rates, for the  $\text{Sn}_5\text{Ge}_{10}\text{Se}_{82.5}\text{Pb}_{2.5}$  chalcogenide glass.

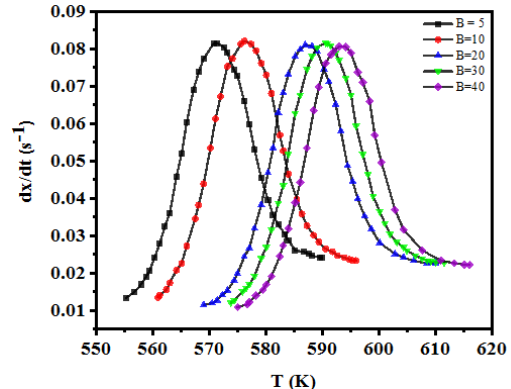


Figure 15. The crystallization rate  $(dx/dt)T$  as a function of temperature, at different heating rates, for the  $\text{Sn}_5\text{Ge}_{10}\text{Se}_{82.5}\text{Pb}_{2.5}$  chalcogenide glass.

Now, it can be use the graph shown in **Fig. 15** to calculate the corresponding values of crystallization rates at a peak temperature of crystallization  $(dx/dt)_p$ . Hence, these data can be used to apply the Gao-Wang relation, which can be written in the following form [26]:

$$\ln(dx/dt)_p = (-E_c/RT_p) + const. \quad (13)$$

Applying the Gao-Wang relation to the obtained thermal analysis data give us the graph shown in **Fig. 16a**. The extracted  $E_c$  value from this graph is equal to 7.228 kJ·mol<sup>-1</sup>, which is recorded in **Table 7**. It is clear that the obtained  $E_c$  value is too small compared to those obtained previously in this article, using the methods of Kissinger and Augis and Bennett. Now, another two methods based on the Gao-Wang idea are applied which are depicted as follows.

**Table 7:** The values of the  $E_c$ ,  $n$  and  $m$  deduced from Gao-Wang method, for the Sn<sub>5</sub>Ge<sub>10</sub>Se<sub>82.5</sub>Pb<sub>2.5</sub> chalcogenide glass.

Composition	$E_c$ - G-W (1 <sup>st</sup> method)	$E_c$ - G-W (2 <sup>nd</sup> method)	$E_c$ - G-W (3 <sup>rd</sup> method)	$n$	$m$
Sn <sub>5</sub> Ge <sub>10</sub> Se <sub>82.5</sub> Pb <sub>2.5</sub>	7.23 kJmol <sup>-1</sup>	277.75 kJ·mol <sup>-1</sup>	277.71 kJ·mol <sup>-1</sup>	3.175 ≈ 3	2

Firstly, the  $(dx/dt)_p$  values using the sigmoid curve are extracted. In this method, we determine the slope of the sigmoid curve  $((dx/dT)_p)$  at the corresponding  $T_p$ . Hence, it can be calculate  $(dx/dt)_p$  by multiplying  $(dx/dT)_p$  by the heating rate;  $((dx/dt)_p = (dx/dT)_p \times \beta)$ . Applying the Gao-Wang relation to the obtained thermal analysis data, the graph shown in **Fig. 16b** is obtained. Hence, using the slope of the obtained figure, it can be determine the  $E_c$  value. The obtained  $E_c$  value was found to be equal 277.75 kJ·mol<sup>-1</sup>. This last  $E_c$  value is recorded in **Table 7**.

Second, using the total area curves shown in **Fig. 16c** the  $(dx/dt)_p$  values can be extracted. In this method, we calculate  $(dx/dt)_p$  by taking the slope of the mentioned curve at  $T_p$ . Hence,  $(dx/dt)_p$  can be calculated using the formula  $(dx/dt)_p = ((\text{The slope at } T_p \cdot \beta) / (\text{total area}))$ . The obtained Gao-Wang graph in this case is shown in **Fig. 16d**. Hence, the value of  $E_c$  can be determined using the slope of the obtained graph. The calculated  $E_c$  value is equal 277.71 kJ·mol<sup>-1</sup>, which is recorded in **Table 7** too. Regarding to the obtained  $E_c$  values from the application of Gao-Wang method, reveal that, the last two values were approximately had the same quantity and agree with those obtained previously using Kissinger and Augis-Bennett methods. This infers that, the last applied two methods are correct.

Now, it can use the  $E_c$  value (277.75 kJ·mol<sup>-1</sup>) deduced from the method of Gao-Wang [26] (the sigmoid curve data) and from the corresponding experimental data of  $(dx/dt)_p$ , to calculate the kinetic parameter  $n$  by using the following relation [26]:

$$(dx/dt)_p = n(0.37 \beta E_c / (RT_p)^2) \quad (14)$$

The  $(dx/dt)_p$  vs.  $\beta / T_p^2$  graph for the Sn<sub>5</sub>Ge<sub>10</sub>Se<sub>82.5</sub>Pb<sub>2.5</sub> chalcogenide glass is shown in **Fig. 17**.

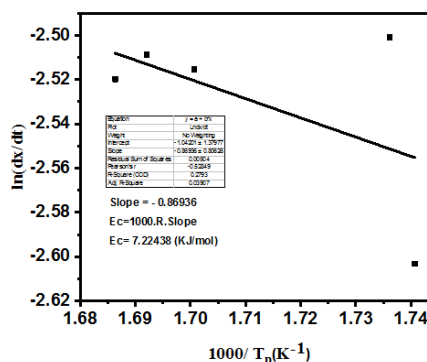


**Figure 16a:** The Gao-Wang  $\ln(dx/dt)_p$  vs.  $1/T_p$  plot for the Sn<sub>5</sub>Ge<sub>10</sub>Se<sub>82.5</sub>Pb<sub>2.5</sub> chalcogenide glass.

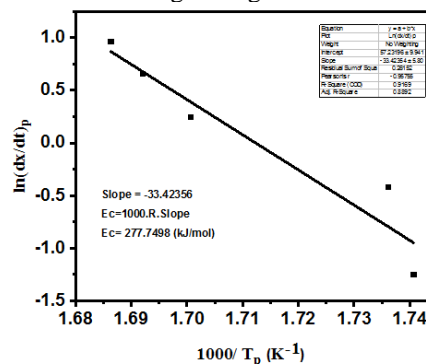


**Fig 16b:** The Gao-Wang  $\ln(dx/dt)_p$  vs.  $1/T_p$  plot, obtained from the sigmoid curve, for the Sn<sub>5</sub>Ge<sub>10</sub>Se<sub>82.5</sub>Pb<sub>2.5</sub> chalcogenide glass.

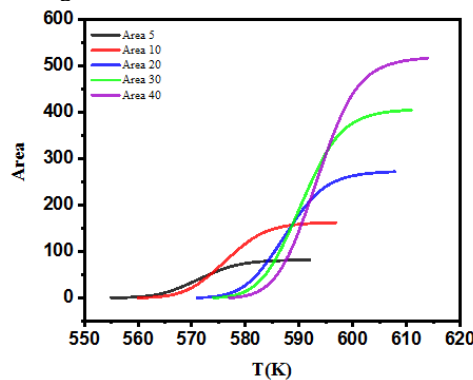


**Fig. 16c:** The total area curves vs.  $T$  for the Sn<sub>5</sub>Ge<sub>10</sub>Se<sub>82.5</sub>Pb<sub>2.5</sub> chalcogenide glass.

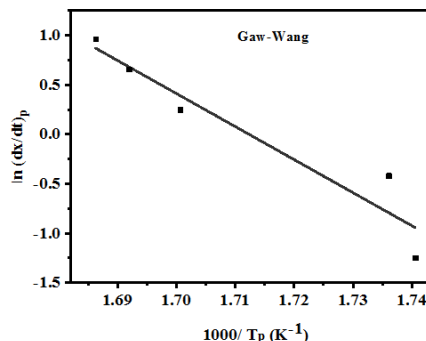


**Fig. 16d:** The Gao-Wang  $\ln(dx/dt)_p$  vs.  $1/T_p$  graph, that obtained from the total area curves, for the Sn<sub>5</sub>Ge<sub>10</sub>Se<sub>82.5</sub>Pb<sub>2.5</sub> chalcogenide glass.

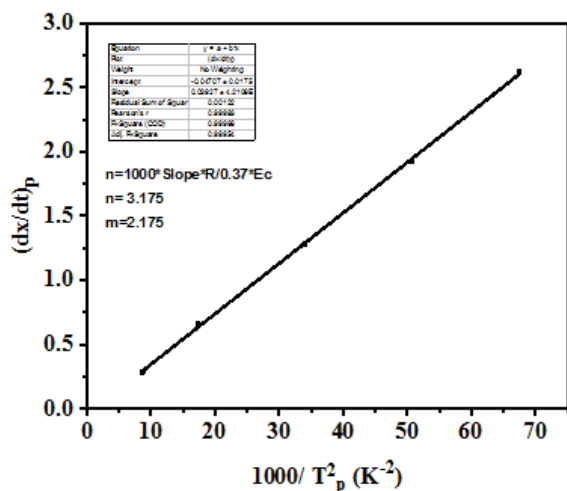


**Figure 17:** The  $(dx/dt)_p$  vs.  $\beta / T_p^2$  graph for the  $\text{Sn}_5\text{Ge}_{10}\text{Se}_{82.5}\text{Pb}_{2.5}$  chalcogenide glass.

The slope of the last figure (Fig. 17) gives us the value of the kinetic parameter  $n = 3.175$ . This value of  $n$  is not integer, which is meant that there is more than one mechanism for crystallization process [25]. In this case it can be approximate  $n = 3$ , then the dimension parameter  $m = 2$ . Accordingly, the crystallization process of the  $\text{Sn}_5\text{Ge}_{10}\text{Se}_{82.5}\text{Pb}_{2.5}$  chalcogenide glass is happen in two-dimensions. This observation may be agreed to the previously calculated  $Z$  data, where the first composition ( $\text{Sn}_5\text{Ge}_{10}\text{Se}_{82.5}\text{Pb}_{2.5}$ ) network has a mechanical threshold or critical composition, at which the network changes from an elastically floppy (polymeric glass) type to a rigid (amorphous solid) type [34, 35]. Besides, this conclusion agreed with the previously calculated fraction of floppy data  $f$  in this text. Where for  $\text{Sn}_5\text{Ge}_{10}\text{Se}_{82.5}\text{Pb}_{2.5}$  glass composition it is observed that, the glass has  $f = 0.04167$  meaning value. When  $x = 5$  at. %,  $f = 0$  and when  $x$  is greater than 5 at. %,  $f$  has no meaningless value.

#### 4. Conclusions

The data from the analysis of thermal transformation were analyzed using a variety of analytical methods. These methods are related to the modified Johnson-Mehl-Avrami formal theory of transformation. The analyses are confined to some standard and more familiar methods, viz; Kissinger, Augis and Bennett, Matusita-Komatsu-Yokota and Gao-Wang methods. The data analysis of the mentioned glasses emphasized that the thermal stability  $\Delta T$  and glass-forming ability  $K_{gl}$  decreased with increased Pb content. On the other side, both  $\Delta T$  and  $K_{gl}$  decreased with the increase of the heating rate  $\beta$  up to 20  $\text{K min}^{-1}$  and then increased with a further increase of  $\beta$ . Besides, the heat changes at glass transition  $\Delta C_p$  and fragility  $F$  decreased with the increase of the heating rate.

#### References

- [1] R.M. Mehra, R. Kumar, and P.c. Mathur, Thin Solid Films 179 (1989) 425.
- [2] N.F. Mott and E.A Davis, Electronic processes in non-Crystalline Materials, Clarendon Press, Oxford, 1979.
- [3] M. M. Wakkad, E. Kh. Shokr and S. H. Mohamed, Phys. Stat. Sol. a 183 (2001) 399.
- [4] J.A. Savage, Infrared Optical Materials and their Antireflection Coatings, Adam Hilger, Bristol, 1985.
- [5] M. M. Wakkad, E. Kh. Shokr and S. H. Mohamed, J. Non-Cryst. Solids 265 (2000) 157.
- [6] A.B. Seddon and M.J. Laine, J. Non- Crystalline Solids, 213 (1997) 168.
- [7] N.F. Mott, E.A. Davis, and R. Street, Phil. Mag. 12 (1975) 961.
- [8] N. Tohge, T. Minami, Y. Yamamoto, and M. Tanaka, J. Appl. Phys. 51 (1980) 1048.
- [9] N. Tohge, H. Matsuo and t. Minami, J. Non- Crystalline Solids, 95 – 96 (1987) 809.
- [10] K.L. Bhatia, S.K. Malik, S. Kishore and S.P Singh, Phil. Mag. B66 (1992) 587.
- [11] B. Vaidhyanathan, S. Murugavel, S. Asokan and K.J. Rao, J. Physical chemistry B., 101 (1997) 9717.
- [12] P. Kumar, V. Mogdil and V.S. Rangra, New Journal of glass and Ceramics, 3 (2013) 116 – 121.
- [13] P. Kumar, V. Modgil and V.S. Rangra, Journal of Non-Oxide Glasses, 6 (2014) 27 – 35.
- [14] S.R. Elliot, Physics of Amorphous Solids, Longman Inc., New York (1984) 134.
- [15] V. Modgil and V.S. Rangra, Journal of Materials, Volume 2014, Article ID 318262 (2014) 1- 8.
- [16] P. Kumar, V. Modgil and V.S. Rangra, Journal of Electronic Materials 45 (2016) 486 – 492.
- [17] P. Kumar, V. Modgil and V.S. Rangra, Journal of Non-Oxide Glasses, 7 (2015) 65 – 81.
- [18] S.R. Elliot, philos. Mag. B36 (1977) 1291.
- [19] M. Lasocka, Mat. Sci. Eng., 23 (1976) 173.
- [20] W.A. Johnson and K.F. Mehl, Transactions of the American Institute of Mining, Metallurgical, Engineers 135 (1939) 416.
- [21] M. Avrami, J. Chem. Phys. 8 (1940) 212.
- [22] M. Avrami, J. Chem. Phys. 9 (1941) 177.
- [23] H.E. Kissinger, J. Res. Nat. Bur. Stand. 57 (1956) 217; Idem, Anal. Chem. 29 (1957) 1702.
- [24] J.A. Augis and J.E. Bennett, J. Thermal Anal. 13 (1978) 283.
- [25] K. Matusita, T. Komatsu and R. Yokota, J. Mater. Sci. 19 (1984) 291.
- [26] Y.Q. Gao, W. Wang, F.Q. Zheng and X. Liu, J. Non- Crystalline Solids, 81 (1986) 135.
- [27] P.S.I. Narasimham, A. Giridhar, S. Mahadevan, J. Non-Crystalline Solids, 43 (1981) 301.
- [28] K. Tanaka, Phys. Rev. B, 39 (1989) 1270.
- [29] L. Tichy, H. Ticha, Mater. Lett. 21 (1994) 313.
- [30] L. Tichy, H. Ticha, J. Non- Crystalline Solids, 189 (1995) 141.
- [31] L. Pauling, The chemical Bond, Cornell University, New York, 1976.

- [32] R.T. Sanderson, *The Chemical Bonds and bond Energy*, academic Press, New York, 1976.
- [33] A.I Allied in S.P. Parker (Ed), *Physical Chemistry Source Book*, McGraw-Hill, New York, (1987) 186.
- [34] M.F. Thorpe, *J. Non- Crystalline Solids*, 57 (1983) 355.
- [35] J.C. Phillips and M.F. Thorpe, *Solid State communication*, 53 (1985) 699.
- [36] S. Mahadevan, A. Giridhar and A.K. Singh, *J. Non- Crystalline Solids*, 88 (1986) 11.
- [37] A. Hruby and L. Stourac, *Mater. Res. Bull.*, 6 (1971) 465.
- [38] C.T. Moynihan and S. Cantor, *J. Chem. Phys.* 48 (1968) 115.
- [39] C.A. Angell, *J. Non- Crystalline Solids*, 73 (1988) 337.
- [40] F.N. Stillinger, *J. Chem. Phys.* 88 (1988) 7818.
- [41] R. Boomer, K.L. Nagi, C.A. Angell and D.G. Plazek, *J. Chem. Phys.* 99 (1993) 4201.
- [42] T.A. Vilgis, *Strong and fragile glasses: A powerful classification and its consequences*, *Physical review B*, 47 (1993) 2882 – 2885.
- [43] R. Boomer, C. Angell, R. Richert and A. Blumen, *Disorder effects of relaxation processes*. Berlin: Springer (1994).
- [44] H. Yinnon and D.R. Uhlmann, *J. Non- Crystalline Solids*, 54 (1983) 253.
- [45] D.W. Handerson, *J. Non- Crystalline Solids*, 30 (1979) 301.
- [46] J. Malek, *Thermochim. Acta.* 267 (1995) 61.
- [47] K. Matusita and S. Sakka, *Phys. Chem. Glasses*, 20 (1979) 81.
- [48] J. Colemenero and J.M. Barandiaran, *J. Non- Crystalline Solids*, 30 (1978) 263.
- [49] R.F. Speyer and S.H. Risbud, *Phys. Chem. Glasses*, 24 (1983) 26.